

Kinetics and Mechanism of the Reduction of Molten Nickel Sulfide by Hydrogen

J. J. BYERLEY, G. L. REMPEL, AND N. TAKEBE

The kinetics and mechanism of the reduction of Ni_3S_2 by hydrogen have been investigated between 1133° and 1300°C. When high flow rates of hydrogen and argon or helium bubbling through the melt are maintained the rate-determining step is a chemical process which can be expressed by a rate law of the form

$$r_{\text{H}_2\text{S}} = k_{\text{expt}} (N_{\text{S}} - \alpha)^2 p_{\text{H}_2}^{1/2}$$

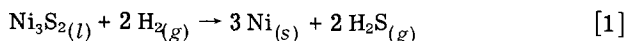
$$p_{\text{H}_2} \geq 0.88 \text{ atm}$$

where $k_{\text{expt}} = 85.1 \text{ atm}^{-1/2} \text{ min}^{-1}$, $\alpha = 0.17$ at 1250°C.

The experimental activation energy for this process is 20.1 ± 3.0 kcal per mole. These results are discussed in terms of possible catalysis by nickel.

REACTIONS between molten metal sulfides and reducing gases have received little attention especially from the kinetic and mechanistic standpoint. Although reactions of this type are not often encountered in metallurgical chemistry, since the conventional route from sulfide to metal consists of a roasting reaction and the subsequent reduction of the oxide to metal, it appears that direct reaction of the sulfide with hydrogen may be promising.

A number of reports on the thermodynamic properties of the binary systems Ni-S, Fe-S, Cu-S¹⁻³ as well as the ternary systems Ni-Fe-S, Ni-Cu-S, and Fe-Cu-S are available.⁴⁻⁶ In many of these investigations the thermodynamic data were obtained by equilibrating an H_2S - H_2 gas mixture with the molten metal sulfide. In this present investigation the kinetics and possible mechanism of the reaction of molten nickel sulfide with hydrogen are reported. The reaction is represented by the following stoichiometry



Data required for a complete kinetic and mechanistic treatment of this reaction were drawn from the related thermodynamic and density studies for the Ni-Fe-S system recently reported by the authors.^{4,7}

EXPERIMENTAL

Theory (General)

The experimental method used in this investigation consisted of direct reaction of the molten nickel sulfide with hydrogen. The rate of sulfur consumption ($-r_{\text{S}}$) was determined by analyzing samples of the sulfide withdrawn periodically from the melt. The rates of hydrogen consumption ($-r_{\text{H}_2}$) and hydrogen sulfide generation ($r_{\text{H}_2\text{S}}$) were obtained from the concentration of these gases in the outlet gas mixture using open system theory.⁸

On the basis of the stoichiometry of the reaction

J. J. BYERLEY, G. L. REMPEL, and N. TAKEBE are with the Metallurgical Chemistry Research Laboratory, Department of Chemical Engineering, University of Waterloo, Waterloo, Ontario, Canada.

Manuscript submitted February 9, 1972.

given in Eq. [1] the following relationship may be written

$$-r_{\text{S}} = -r_{\text{H}_2} = r_{\text{H}_2\text{S}} \quad [2]$$

Modifying open system theory for the case of complete mixing in a stirred flow reaction as discussed by Denbigh *et al.*,⁸ $r_{\text{H}_2\text{S}}$ and r_{H_2} may be expressed as follows

$$r_{\text{H}_2\text{S}} = \frac{dC_{\text{H}_2\text{S}}}{dt} + \frac{U}{V(t)} C_{\text{H}_2\text{S}} \quad [3]$$

$$-r_{\text{H}_2} = \frac{dC_{\text{H}_2}}{dt} + \frac{U}{V(t)} (C_{\text{H}_2} - C'_{\text{H}_2}) \quad [4]$$

$$V(t) = \frac{M(t)}{D(t)} = \frac{M(S)}{D(S)} \quad [5]$$

where

$C_{\text{H}_2\text{S}}$ = hydrogen sulfide concentration in outlet gas mixture

C_{H_2} = hydrogen concentration in outlet gas mixture

C'_{H_2} = hydrogen concentration in inlet gas mixture

U = inlet gas flow rate

$V(t)$ = molten nickel sulfide volume (variable with time)

$M(t)$ = molten nickel sulfide weight (variable with time)

$D(t)$ = molten nickel sulfide density (variable with time)

$M(S)$ = molten nickel sulfide weight (variable with sulfur content)

$D(S)$ = molten nickel sulfide density (variable with sulfur content)

At steady-state dC/dt is zero and the basic equations become

$$r_{\text{H}_2\text{S}} = \frac{U}{V(t)} C_{\text{H}_2\text{S}} \quad [6]$$

$$-r_{\text{H}_2} = \frac{U}{V(t)} (C_{\text{H}_2} - C'_{\text{H}_2}) \quad [7]$$

Eqs. [6] and [7] give the rate of hydrogen sulfide generation and hydrogen consumption as a function of the concentrations of the gases in the outlet gas mixture, the sulfur content of the nickel sulfide and the density of the molten nickel sulfide.⁷

Materials

The nickel sulfide was prepared by heating pure nickel powder (99.79 pct purity) with reagent grade sulfur in a high-purity recrystallized alumina crucible. All fusions were done under purified argon. The nickel was carbonyl nickel powder 128 supplied by the International Nickel Company of Canada Ltd. Argon, hydrogen, helium, and hydrogen sulfide were supplied by Matheson of Canada Ltd. Sulfur was supplied by British Drug House.

The composition of synthetic nickel sulfide was determined to be 73.29 wt pct Ni and 26.71 wt pct S which is very near the stoichiometric composition of Ni₃S₂ (73.24 wt pct Ni, 26.76 wt pct S).*

*For experiments using He-H₂ mixtures (data, Fig. 8) the nickel sulfide composition was 74.58 wt pct Ni and 25.42 wt pct S.

Experimental Apparatus

The apparatus consisted of a furnace, gas flow-meters, gas purification system, molten sulfide container, quartz stirring rod and propeller, and gas chromatograph. The furnace was a vertical silicon carbide resistance type capable of operation up to 1500°C with a constant temperature zone of about 15 cm. The furnace was controlled to within ±2°C using a standard controller activated by a Pt-Pt 13 pct Rh thermocouple. The furnace temperature was monitored with a calibrated Pt-Pt 13 pct Rh thermocouple. The gas purification system consisted of a palladinized asbestos tube, two pyrogallol columns, four calcium chloride columns and three silica gel columns. The crucible containing the molten nickel sulfide was high-purity recrystallized alumina measuring 9 cm long with an ID of 3.8 cm. The quartz stirring rod was 3 mm in diameter and 50 cm long. This rod was connected to a variable speed motor (0 to 100 rpm).

Procedure

Between 55 and 70 g of nickel sulfide was fused in an alumina crucible under purified argon. When the desired temperature was reached the quartz stirring rod was activated and purified hydrogen was bubbled through the molten nickel sulfide. The progress of the reaction was followed by periodic sampling and analysis of both the outlet gas mixture and nickel sulfide. The gas analysis was done with an F and M Scientific Corporation Model 700 gas chromatograph using Porapak Q and Molecular Sieve Type 5A columns. The nickel sulfide was analyzed for sulfur using a standard gravimetric method.

EXPERIMENTAL RESULTS

Profile of the Reaction

In Fig. 1 typical experimental data are given showing the consumption of sulfur in the nickel sulfide, the consumption of hydrogen, and the generation of hydro-

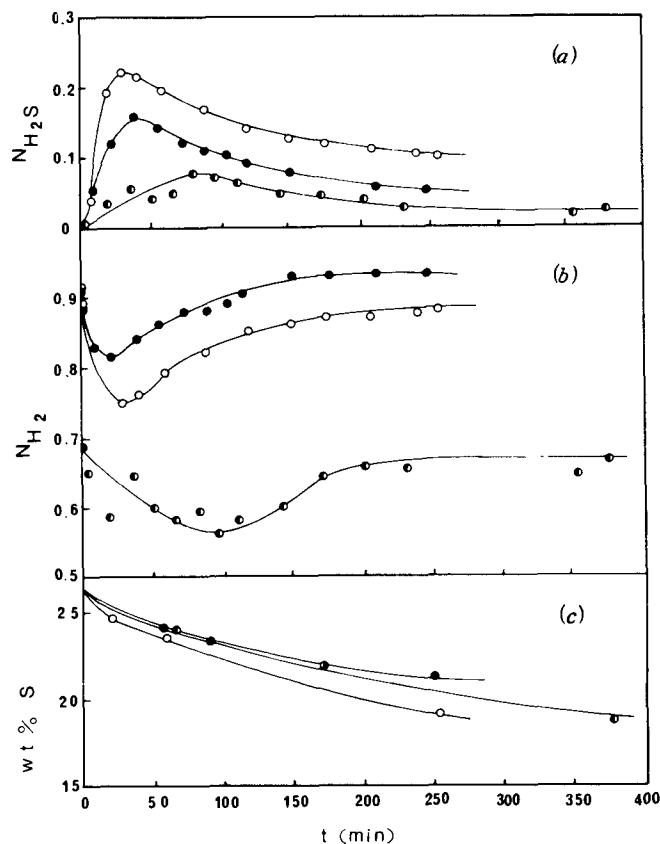


Fig. 1—Typical experimental curves. (a) Profile of hydrogen sulfide generation with time. (b) Profile of hydrogen consumption with time. (c) Profile of sulfur consumption with time.

○ Temp = 1247°C, gas flow rate = 200 cu cm per min, p_{H_2} = 0.918 atm, bubbling, stirring rate = 65 rpm, sample = 70 g.
● Temp = 1133°C, gas flow rate = 178 cu cm per min, p_{H_2} = 0.901 atm, bubbling, stirring rate = 65 rpm, sample = 70 g.
◐ Temp = 1250°C, gas flow rate = 196 ± 3 cu cm per min, p_{H_2} = 0.680 atm, bubbling, no stirring, sample = 55 g.

gen sulfide as a function of time. The shape of these curves was characteristic of all experiments.

The first observable indication of reaction took place about 5 min after introduction of hydrogen. The maximum hydrogen sulfide and maximum hydrogen consumption rates occur from 30 to 60 min after the start of the reaction. Fig. 2 shows the hydrogen sulfide generation rate as a function of sulfur content of the nickel sulfide for three experiments. These curves may be considered in two sections. Section 1 corresponds to the period from the beginning of the reaction to a steady-state condition. Section 2 corresponds to the steady state. For the purposes of this discussion only the steady-state portion of the reaction is significant.

Kinetics of the Reaction

a) EFFECT OF MELT GEOMETRY AND AGITATION

Experiments were carried out to investigate the effect of melt geometry, stirring, and inlet gas flow rate. Two experiments were performed using 70 and 55 g samples. The results given in Fig. 3 show that sample size has little effect on the reaction rate.

Two experiments were carried out using stirring of

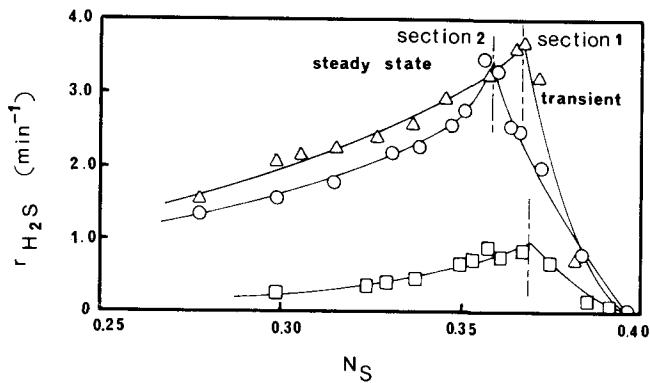


Fig. 2—Hydrogen sulfide generation rate vs N_S . \circ Temp = 1250°C, gas flow rate = 200 ± 10 cu cm per min, p_{H_2} = 0.901 atm, bubbling, no stirring, sample = 70 g. Δ Temp = 1247°C, gas flow rate = 200 cu cm per min, p_{H_2} = 0.918 atm, bubbling, stirring rate = 65 rpm, sample = 70 g. \square Temp = 1250°C, gas flow rate = 105 cu cm per min, p_{H_2} = 0.681 atm, bubbling, no stirring, sample = 55 g.

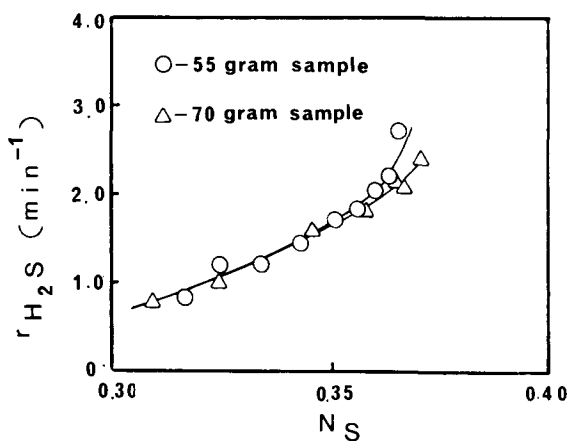


Fig. 3—Effect of melt geometry. Temp = 1249°C, gas flow rate = 186 ± 9 cu cm per min, p_{H_2} = 0.738 atm, bubbling, no stirring.

0 and 65 rpm. The effect of changing stirring rates on the rate of reaction was rather minor as shown in Fig. 4. However, it is important to recognize that the melt is also agitated quite violently by the bubbling H_2 -Ar gas mixture. Thus the effect of inlet gas bubbling must be considered before the nature of the rate limiting step can be identified.

Fig. 5 shows the effect of inlet gas ($H_2 + Ar$) flow rate on the reaction rate at a constant H_2/Ar ratio of approximately 2. The results indicate that at a flow rate of over 200 cu cm per min the reaction is rather insensitive to variation in flow rate while at lower flow rates the reaction rate varies with flow rate. These observations coupled with those involving melt geometry would suggest that the reaction mechanism is essentially independent of diffusion at high flow rate and may be dependent on diffusion at low flow rate.

b) EFFECT OF SULFUR CONTENT

Examination of r_{H_2S} vs N_S curves shown in Fig. 2 indicates a major dependence of reaction rate on the sulfur content of the molten nickel sulfide. Although a plot of r_{H_2S} vs N_S^2 , did show linearity indicative of second-order kinetics, extrapolation into the low sul-

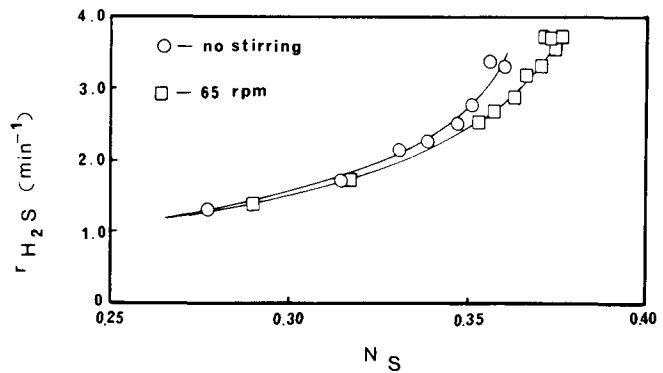


Fig. 4—Effect of stirring rate. Temp = 1250°C, gas flow rate = 200 ± 10 cu cm per min, p_{H_2} = 0.901 atm, bubbling, sample = 70 g.

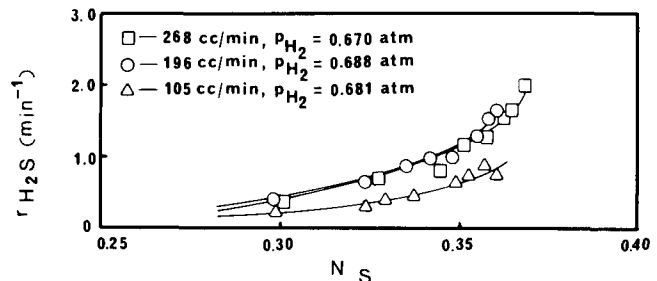


Fig. 5—Effect of gas flow rate. Temp = 1250°C, bubbling, no stirring, sample = 55 g.

fur region resulted in a nonzero intercept. Fig. 6 shows plots of r_{H_2S} vs $(N_S - \alpha)^2$ where $\alpha = 0.17$ at 1250°C. These curves are linear and do extrapolate to the origin. This relationship suggests a second-order dependence on sulfur in the range of sulfur concentration and hydrogen pressure investigated. The value of α at 1250°C corresponds to the sulfur content of the sulfide at the point where nickel separates from the sulfide ($N_S = 0.17$).⁹ Examination of the reaction in the vicinity of $N_S = 0.17$ resulted in H_2S evolution rates that were so low as to be virtually immeasurable. This apparent change in kinetic behavior can be attributed to the appearance of a new less reactive sulfide which may exhibit less than second-order kinetics with respect to the sulfur concentration. Second-order kinetics above $N_S = 0.17$ still remain valid. Some further comments on the role of sulfur in the reaction are given in the Discussion section.

c) EFFECT OF HYDROGEN PRESSURE

Experiments were conducted using different partial pressures of hydrogen while maintaining a constant flow rate above 200 cu cm per min. An increase in hydrogen partial pressure has a marked effect on the rate of reaction as shown by the series of curves in Fig. 6. In Fig. 7 the slopes obtained from Fig. 6 are plotted vs $p_{H_2}^{1/2}$. A linear relationship is obtained in the pressure range 0.88 to 1.03 atm (total pressure 1.00 to 1.06 atm). Below $p_{H_2} = 0.88$ atm the linear relationship is no longer valid.

d) EFFECT OF INERT GAS

In order to determine whether the hydrogen pressure dependence observed was in fact genuine, three

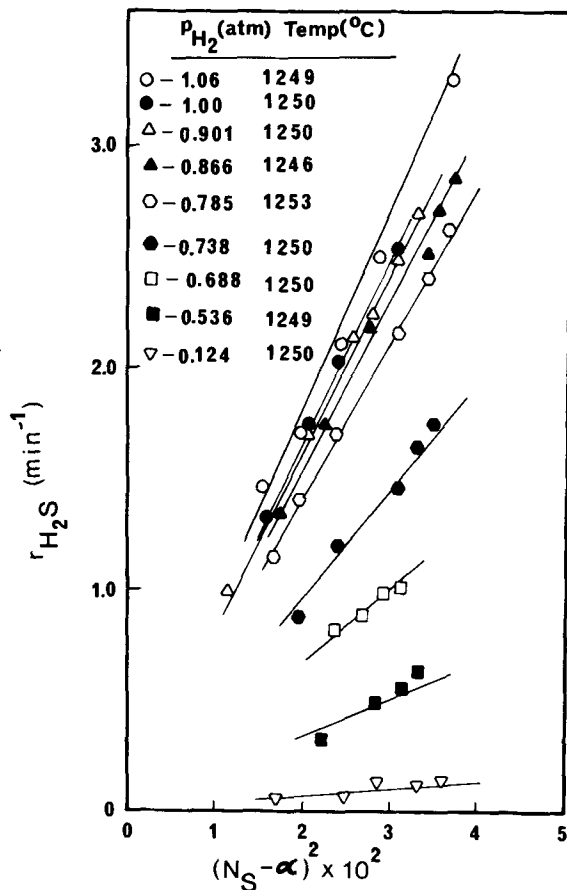


Fig. 6—Dependence of reaction rate on sulfur content and hydrogen pressure. Gas flow rate = 186 – 268 cu cm per min, bubbling, no stirring, sample = 55 – 70 g.

experiments were performed in which H₂-He gas mixtures were substituted for H₂-Ar gas mixtures. In these experiments only chemical analysis of the molten sulfide with time was done because the chromatographic separation of H₂ and He was unreliable. The data obtained from these experiments are summarized in Fig. 8. The $r_{H_2S}/(N_S - \alpha)^2$ values calculated from the data given in Fig. 8 are included in Fig. 7. The rates are seen to be unaffected by the different hydrogen-inert gas mixture at high partial pressures of hydrogen. As the partial pressure of hydrogen is reduced the rate of reaction for H₂-Ar mixtures is larger than the rate for H₂-He mixtures under comparable conditions. These observations lend support to the validity of the half-order hydrogen dependence of the reaction rate at a high partial pressure of hydrogen while indicating that a transport process may have increasing significance at lower hydrogen partial pressure. This phenomenon was not further examined due to difficulty in obtaining reliable data at low hydrogen partial pressures although some speculation on the effect is given in the Discussion section.

Rate Law Formulation

In view of the observed effects of sulfur concentration and hydrogen partial pressure on the hydrogen sulfide generation rate, the experimental rate law may be formulated as follows

$$r_{H_2S} = k_{\text{expt}} (N_S - \alpha)^2 p_{H_2}^{1/2} \quad [8]$$

where

$$\alpha = 0.17 \text{ at } 1250^\circ\text{C}$$

$$k_{\text{expt}} = 85.1 \text{ atm}^{-1/2} \text{ min}^{-1} \text{ at } 1250^\circ\text{C}$$

This rate law is valid for partial pressures of hydrogen above 0.88 atm (total pressure = 1.00 to 1.06 atm).

Effect of Temperature

The effect of temperature was investigated over the temperature range 1133° to 1300°C using a hydrogen

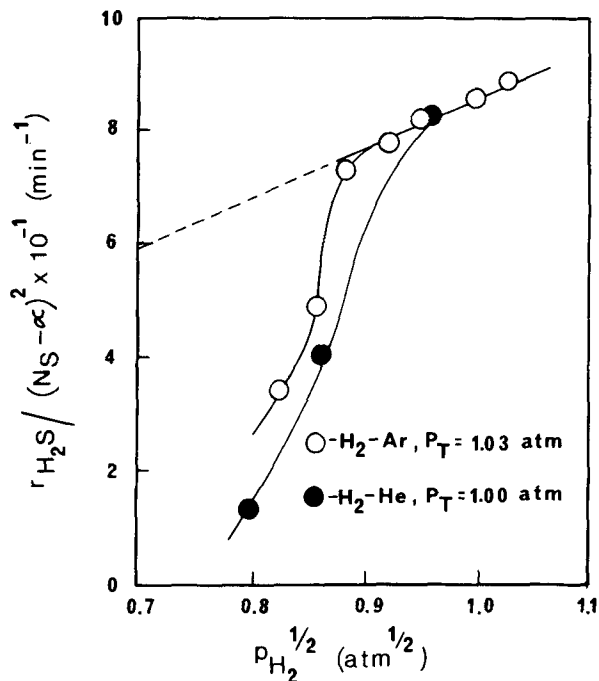


Fig. 7— $r_{H_2S}/(N_S - \alpha)^2$ vs $p_{H_2}^{1/2}$ plot. Temp = 1246°C to 1253°C, gas flow rate = 186 to 268 cu cm per min, bubbling, no stirring, sample = 55 to 70 g.

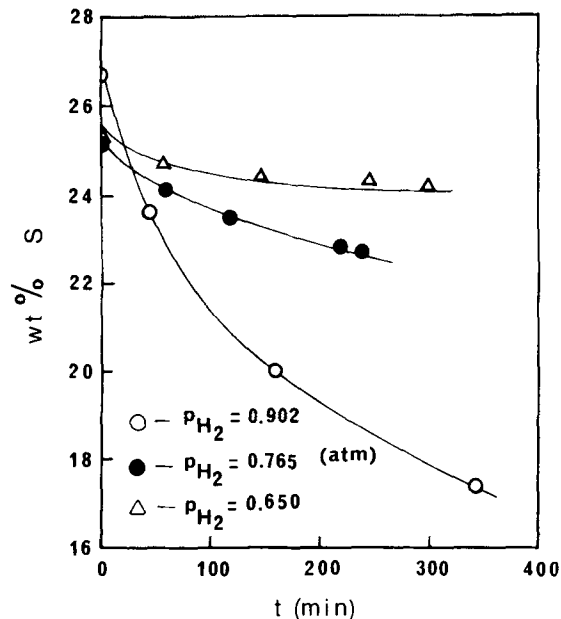


Fig. 8—Experimental results with H₂-He gas mixture. Total pressure = 1.00 atm, temp = 1250°C, gas flow rate = 198 to 202 cu cm per min, bubbling, no stirring, sample = 70 g.

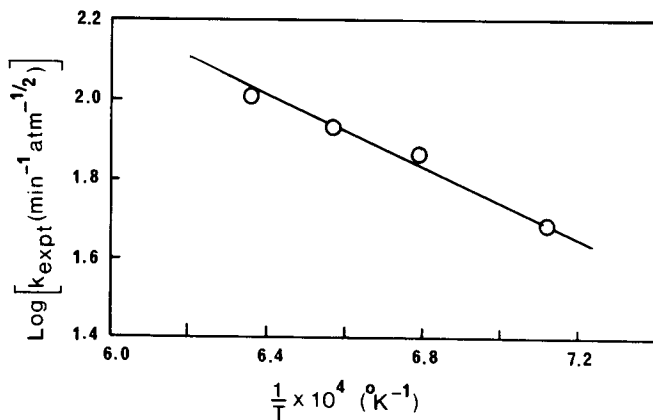


Fig. 9—Arrhenius plot. Gas flow rate = 190 ~ 200 cu cm per min, p_{H_2} = 0.901 to 0.905 atm, bubbling, stirring rate = 65 rpm, sample = 70 g.

partial pressure of 0.901 to 0.905 atm (total pressure \approx 1.00 atm). From the Arrhenius plot shown in Fig. 9 an experimental activation energy of 20.1 ± 3.0 kcal per mole was calculated. This value falls within the range generally found for a chemically controlled process.

DISCUSSION

A reaction mechanism may be postulated which is compatible with the kinetic evidence summarized in the rate law given by Eq. [8]. The mechanism may be represented by the following scheme:



The rate law derived from this reaction sequence corresponds to

$$r_{\text{H}_2\text{S}} = \frac{k_c K_1^{1/2} K_2^{1/2} \gamma_3}{\gamma_1 \gamma_2^{1/2}} N_{\text{S}}^2 p_{\text{H}_2}^{1/2} \quad [13]$$

where

$$a_{\text{H}} = \gamma_1 N_{\text{H}} \quad [14]^*$$

*Henry's Law relationship.

$$a_{\text{S}_2} = \gamma_2 N_{\text{S}_2}^2 \quad [15]^\dagger$$

$$a_{\text{S}} = \gamma_3 N_{\text{S}}^2 \quad [16]^\dagger$$

†Expressions based on activity data obtained for the Ni-S system.⁴

The rate expression derived from the reaction mechanism is consistent with the experimental rate law if:

$$N_{\text{S}} = N_{\text{S}} - \alpha \quad [17]$$

and

$$k_{\text{expt}} = \frac{k_c K_1^{1/2} K_2^{1/2} \gamma_3}{\gamma_1 \gamma_2^{1/2}} \quad [18]$$

The equilibrium shown in Eq. [9] is proposed because diatomic gases such as H_2 are considered to exist in solution of molten metals in monatomic form (Sie-

Table I. Effect of Nickel on the Activation Energy of Some Reactions Involving Hydrogen^{11,13,14}

Reaction	E_{Ni}^* kcal per mole	E kcal per mole
$\text{H}_2 \longrightarrow 2\text{H}$	0.5	100
$\text{H}_2 + \text{D}_2 \longrightarrow 2\text{HD}$	8	90
$\text{C}_2\text{H}_4 + \text{H}_2 \longrightarrow \text{C}_2\text{H}_6$	~ 9	43
$\text{C}_6\text{H}_6 + \text{H}_2 \longrightarrow \text{C}_6\text{H}_8$	11	78
$\text{H}_2 + \text{S} \longrightarrow \text{H}_2\text{S}$	20†	45

* E_{Ni} denotes activation energy in the presence of nickel.

†Present work.

vert's Law).¹⁰ In the present case it seems reasonable to assume that this might be applicable to a sulfide melt. Eq. [10] represents an equilibrium suggested on the basis of the results of Aynsley *et al.*¹¹ for the reaction between hydrogen and sulfur at 350°C.

The experimental activation energy associated with the above suggested mechanism was calculated to be 20.1 ± 3.0 kcal per mole. This value is about 25 kcal per mole less than the value for the hydrogen-liquid sulfur or hydrogen-gaseous sulfur reactions reported by Aynsley *et al.*¹¹ This difference is easily explained by consideration of the nature of the reacting species in the rate determining step.

In the mechanistic scheme shown above the rate determining step involves a reaction between S_2 and H in the melt. Consideration of the molecular orbitals of these two species suggests that this reaction is symmetry allowed.¹² However, the rate-determining step for the hydrogen-liquid sulfur reaction is symmetry forbidden. It appears that the nickel present in Ni_3S_2 may be functioning as a catalyst by promoting step one in the above mechanistic scheme. Consequently the H species in the rate-determining step may be that of an adsorbed type.

The role of nickel metal as a catalyst for hydrogen activation is well-known¹³ and it is conceivable that nickel present in molten Ni_3S_2 may exhibit, at least to some extent, similar properties. Some activation energy data for reactions involving hydrogen in the presence and absence of nickel are given in Table I. The primary function of the catalyst is to adsorb the reacting molecules, with the result that the reaction may occur via a path involving a lower activation energy.¹⁴ The application of quantum mechanics to a system containing a hydrogen molecule and two surface atoms of nickel has led to the conclusion that in the most stable configuration the distance between the adsorbed hydrogen atoms is much greater than in the normal H_2 molecules.¹⁵ Thus, adsorption is accompanied by dissociation of the adsorbed molecule which is consistent with the monatomic nature of dissolved hydrogen in molten metals.¹⁰

A possible explanation of the effect of inert gas on the reaction rate may be that the gas molecules participate in the desorption of hydrogen sulfide formed in the fast step of the reaction mechanism. There are several reports¹⁶⁻¹⁸ which describe the effects of inert gases on rates and activation energies of gas-solid reactions. The explanation generally given is based on a momentum exchange between the inert gas and adsorbed molecule. In the present case it is difficult to say without more experimental data whether an explanation of

this type is applicable to a gas-liquid reaction.

The apparent shift in kinetics from second order in sulfur to some lower dependence below $N_S = 0.17$ can be discussed qualitatively in terms of known sulfur activity. From thermodynamic data for the Ni-S^{1,2,3,4} system the activity of sulfur in nickel sulfide decreases parabolically as the sulfur concentration decreases. For example at 1250°C the sulfur activity and activity coefficient defined as p_{H_2S}/p_{H_2} , $(p_{H_2S}/p_{H_2})/N_S$ are 5×10^{-1} and 1.54 for $N_S = 0.325$ whereas for $N_S = 0.17$, the sulfur activity and activity coefficient are 5×10^{-3} and 2.94×10^{-2} respectively. The rather sharp decrease in sulfur activity as the sulfur concentration nears the value for phase separation would indicate that the interaction energy for Ni-S is increasing while the interaction energy for Ni-Ni and S-S is decreasing. Although there are undoubtedly other factors which contribute to the observed kinetics with respect to sulfur concentration in the melt it is not unreasonable to relate sulfur activity and interaction energies of constituents with the change in kinetics observed for the desulfurization rate of the nickel sulfide.

ACKNOWLEDGMENT

The authors are grateful to the National Research Council of Canada for financial assistance and the In-

ternational Nickel Company of Canada Ltd. for supplying materials used in this project.

REFERENCES

1. M. Nagamori and T. R. Ingraham: *Met. Trans.*, 1970, vol. 1, pp. 1821-25.
2. T. Rosenqvist: *J. Iron Steel Inst.*, 1954, vol. 174, p. 37.
3. R. Schuhmann, Jr. and O. W. Moles: *AIME Trans.*, 1951, vol. 191, pp. 235-41.
4. J. J. Byerley and N. Takebe: *Met. Trans.*, 1972, vol. 3, pp. 559-64.
5. J. W. Matousek and C. S. Samis: *Trans. TMS-AIME*, 1963, vol. 227, pp. 980-85.
6. W. A. Krivsky and R. Schuhmann, Jr.: *AIME Trans.*, 1957, vol. 209, pp. 981-88.
7. J. J. Byerley and N. Takebe: *Met. Trans.*, 1971, vol. 2, pp. 1107-11.
8. K. G. Denbigh, M. Hicks, and F. M. Page: *Trans. Faraday Soc.*, 1948, vol. 44, pp. 479-94.
9. M. Hansen: *Constitution of Binary Alloys*, McGraw-Hill, New York, N. Y., 1958, pp. 1034-36.
10. L. S. Darken and R. W. Gurry: *Physical Chemistry of Metals*, McGraw-Hill, New York, N. Y., 1953, pp. 132-33.
11. E. E. Aynsley, T. G. Pearson, and P. L. Robinson: *J. Chem. Soc.*, 1935, pp. 58-68.
12. R. G. Woodward and R. Hoffman: *The Conservation of Orbital Symmetry*, Academic Press, New York, N. Y., 1969.
13. G. C. Bond: *Catalysis by Metals*, Academic Press, New York, N. Y., 1962.
14. G. Glasstone, K. J. Laidler, and H. Eyring: *The Theory of Rate Processes*, McGraw-Hill, New York, N. Y., 1941.
15. A. Sherman, C. E. Sun, and H. Eyring: *J. Chem. Phys.*, 1935, vol. 3, pp. 49-55.
16. T. Baron, W. R. Manning, and H. F. Johnstone: *Chem. Eng. Progr.*, 1952, vol. 48, pp. 125-32.
17. A. A. Yeramian, P. L. Silveston, and R. R. Hudgins: *Can. J. Chem.*, 1970, vol. 48, pp. 1175-82.
18. W. G. Rhodery: M. A. Sc. Thesis, University of Waterloo, 1969.